



Intravascular Molecular Imaging: Near-Infrared Fluorescence as a New Frontier

Haitham Khraishah^{1,2} and Farouc A. Jaffer^{2,3*}

¹ Department of Medicine, Beth Israel Deaconess Medical Center and Harvard Medical School, Boston, MA, United States,

² Division of Cardiology, Cardiovascular Research Center and Harvard Medical School, Massachusetts General Hospital, Boston, MA, United States, ³ Wellman Center for Photomedicine and Harvard Medical School, Massachusetts General Hospital, Boston, MA, United States

OPEN ACCESS

Edited by:

Xiaowei Wang,
Baker Heart and Diabetes
Institute, Australia

Reviewed by:

Jinwei Tian,
Second Affiliated Hospital of Harbin
Medical University, China
Amir Rosenthal,
Technion Israel Institute of
Technology, Israel
Antonios Karanasos,
Hippokraton General Hospital, Greece

*Correspondence:

Farouc A. Jaffer
fjaffer@mgh.harvard.edu

Specialty section:

This article was submitted to
Cardiovascular Imaging,
a section of the journal
Frontiers in Cardiovascular Medicine

Received: 24 July 2020

Accepted: 30 October 2020

Published: 23 November 2020

Citation:

Khraishah H and Jaffer FA (2020)
Intravascular Molecular Imaging:
Near-Infrared Fluorescence as a New
Frontier.
Front. Cardiovasc. Med. 7:587100.
doi: 10.3389/fcvm.2020.587100

Despite exciting advances in structural intravascular imaging [intravascular ultrasound (IVUS) and optical coherence tomography (OCT)] that have enabled partial assessment of atheroma burden and high-risk features associated with acute coronary syndromes, structural-based imaging modalities alone do not comprehensively phenotype the complex pathobiology of atherosclerosis. Near-infrared fluorescence (NIRF) is an emerging molecular intravascular imaging modality that allows for *in vivo* visualization of pathobiological and cellular processes at atheroma plaque level, including inflammation, oxidative stress, and abnormal endothelial permeability. Established intravascular NIRF imaging targets include macrophages, cathepsin protease activity, oxidized low-density lipoprotein and abnormal endothelial permeability. Structural and molecular intravascular imaging provide complementary information about plaque microstructure and biology. For this reason, integrated hybrid catheters that combine NIRF-IVUS or NIRF-OCT have been developed to allow co-registration of morphological and molecular processes with a single pullback, as performed for standalone IVUS or OCT. NIRF imaging is approaching application in clinical practice. This will be accelerated by the use of FDA-approved indocyanine green (ICG), which illuminates lipid- and macrophage-rich zones of permeable atheroma. The ability to comprehensively phenotype coronary pathobiology in patients will enable a deeper understanding of plaque pathobiology, improve local and patient-based risk prediction, and usher in a new era of personalized therapy.

Keywords: intravascular imaging, atherosclerotic cardiovascular disease, optical coherence tomography, molecular imaging, near-infrared fluorescence (NIRF)

INTRODUCTION

In 1989, Muller et al. (1) proposed the term “vulnerable plaque” to describe coronary artery plaques prone to rupture and cause acute myocardial infarction or sudden cardiac death. In 2003, a group of experts reached a consensus on a definition of vulnerable/high risk plaque being “a plaque that is at increased risk of thrombosis (or recurrent thrombosis) and rapid stenosis progression” (2). This definition extends beyond plaque rupture to include disruptions that may also occur from plaque erosions and penetrating calcified nodules. In general, the current paradigm of a high-risk plaque involves a thin cap fibroatheroma (TCFA), characterized by a large,

necrotic, lipid-rich core and an overlying thin fibrous cap of $<65\ \mu\text{m}$ thickness. Other high risk features include inflammation, microcalcifications, neovascularization, intraplaque hemorrhage and positive remodeling (3–5).

High-resolution intravascular imaging modalities, such as intravascular ultrasound (IVUS) and optical coherence tomography (OCT), assess *in vivo* atheroma burden and some high-risk features reflecting plaque vulnerability (6). Despite these advances, current anatomical intracoronary imaging modalities have their shortcomings in predicting future acute coronary syndrome (ACS) events, even when incorporating advanced IVUS-derived high risk plaque measures, such as high plaque burden $>70\%$, minimal luminal area $<4\ \text{mm}^2$, IVUS-virtual histology demarcated TCFA, and low endothelial shear stress (7–9). To address the limitations of anatomical intracoronary imaging, near-infrared fluorescence (NIRF) molecular imaging has emerged as a translational intravascular modality that allows visualization of plaque pathobiology by targeting certain molecular processes through specialized imaging agents [fluorophore-conjugates (10, 11) or protease-activatable constructs (12, 13) for example]. No single modality allows for the comprehensive evaluation of a plaque; to meet this need, hybrid catheters that allow co-registration of images acquired by different modalities have been developed. The aim of this review is to showcase the latest developments in molecular intravascular imaging, with a focus NIRF hybrid imaging modalities, and delve into current limitations and future prospects.

PLAQUE PATHOBIOLOGY

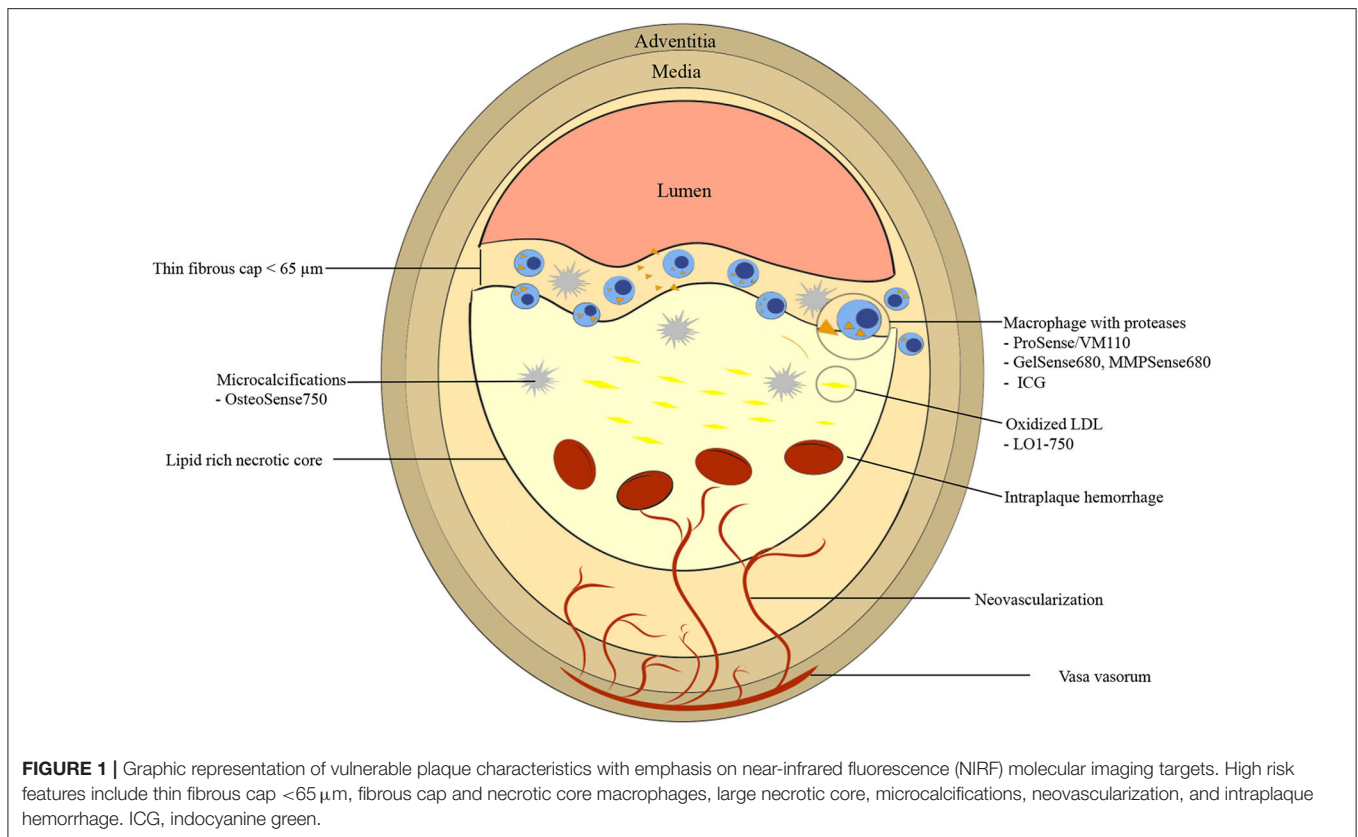
The underlying pathobiology of atherosclerosis provides a roadmap for molecular imaging targets and imaging agent synthesis (Figure 1). Atherosclerosis is a chronic inflammatory disease characterized by endothelial dysfunction, arterial wall thickening and persistent immune activation. An initial step in atherogenesis is vascular endothelial dysfunction, triggered by an increase in oxidative stress within a milieu of hyperlipidemia, hyperglycemia, smoking and hypertension (14). Small low-density lipoprotein (LDL) particles infiltrate through the impaired endothelial barrier and accumulate in the subendothelial matrix (15, 16). Oxidized LDL (oxLDL) is internalized by local macrophages giving rise to foam cells (17–19). Vascular smooth muscle cells (VSMCs) migrate from the tunica media to intima in response to inflammatory mediators, growth factors, and cytokines. There, they proliferate and secrete extracellular matrix including proteoglycans and collagen type 2, contributing to plaque stability through the formation of a fibrous cap (20, 21). Apoptosis and necrosis of activated macrophages and VSMCs results in the formation of a lipid-rich necrotic core that is encapsulated by collagen-rich fibrous tissue, a fibrous cap (18, 22). When a fibroatheroma exists under a thin fibrous cap (thinned by inflammatory proteases such as MMPs and cathepsins), these advanced lesions are denoted as TCFAs, the current paradigm of high-risk plaque.

Another high-risk plaque feature is microcalcification. Calcification is an active process that occurs during all stages of atherosclerosis. Macrocalcifications, which are detectable by CT scan due to high radiodensity [>400 Hounsfield unit (HU)], may be associated with more stable plaque phenotypes (23). In contrast, microcalcifications (<0.05 to $15\ \mu\text{m}$) are undetectable by conventional imaging modalities and may have a destabilizing effect on fibroatheromas (24). When microcalcifications, arise within the fibrous cap, local stress increases by 2-fold, putatively contributing to plaque vulnerability (25). Microcalcification-aggregation results in macrocalcifications (18). Another high-risk vulnerable plaque feature is spotty calcifications, small calcium deposits that can be detected via OCT, IVUS, and CT. For IVUS and OCT, spotty calcification is defined as a calcium length $<4\ \text{mm}$ and a maximal calcium angle ranging from 22.5 to 90° (26). For CT, spotty calcifications are typically defined as average density >130 HU, diameter $<3\ \text{mm}$ in any direction, length of the calcium $<1.5\times$ the vessel diameter, and width of the calcification less than two-thirds of the vessel diameter (27).

Positive remodeling is thought to contribute to plaque instability by induction of neovascularization of vasa vasorum in the adventitia that eventually invade the intima and the fibroatheroma (28). These new microvessels have fragile walls leading to intraplaque hemorrhage (resulting in plaque expansion and pro-inflammatory milieu), and express adhesion molecules recruiting further macrophages into the plaque (Figure 1) (29).

DETECTING HIGH RISK PLAQUE: SIGNIFICANCE, CHALLENGES, AND INTRAVASCULAR IMAGING

The goal of detecting high-risk plaques is to identify rupture-prone plaques and intervene in a way (either medically or interventional or both) to prevent future ACS. Very recently, the COMPLETE trial showed that in patients with STEMI and multivessel coronary artery disease (CAD), intervening on non-culprit lesions reduced a composite of CVD death and myocardial infarction (30), demonstrating the potential to identify a subgroup of high-risk, non-culprit lesions (admittedly a proportion of these lesions may have been flow-limiting and met common indications for revascularization, independently of the COMPLETE trial). However, in other clinical scenarios such as stable CAD, several challenges exist as to which non-culprit lesions to intervene upon. These challenges are due to imprecise knowledge of the natural history of plaque progression based on structural-based imaging trials and autopsy studies. Also, coronary artery plaques are of dynamic nature with lesion morphology oscillating from high risk to more stable and vice versa over time, as demonstrated by small longitudinal imaging studies (31–33). Additionally, current anatomical intravascular imaging modalities have limited ability to predict ACS arising from high risk plaques. In the PROSPECT trial, after incorporating all IVUS-derived predictive variables [high plaque burden $>70\%$, minimal luminal area <4 square mm, or



IVUS-virtual histology demarcated thin capped fibroatheroma (TCFA)], IVUS was limited in forecasting event-causing lesions with a relatively low positive predictive value (PPV) of 18.2% (meaning 4 out of 5 three-feature plaques did not produce in an event at 3 years) (9). Integrating endothelial shear stress parameters in the PREDICTION trial enhanced PPV to 41% (7), which is an improvement but still insufficient for routine clinical management. Therefore, new imaging approaches to more comprehensively phenotype atheroma are needed to improve lesion-specific risk prediction.

INTRAVASCULAR MOLECULAR IMAGING

To tackle the limitations of anatomical intravascular imaging modalities, intravascular molecular imaging has been developed to allow for *in vivo* visualization of molecular process that contribute to plaque vulnerability. The primary intravascular molecular imaging modality nearing clinical translation utilizes near infrared fluorescence (NIRF) detection of targeted NIR fluorophores, discussed in detail next.

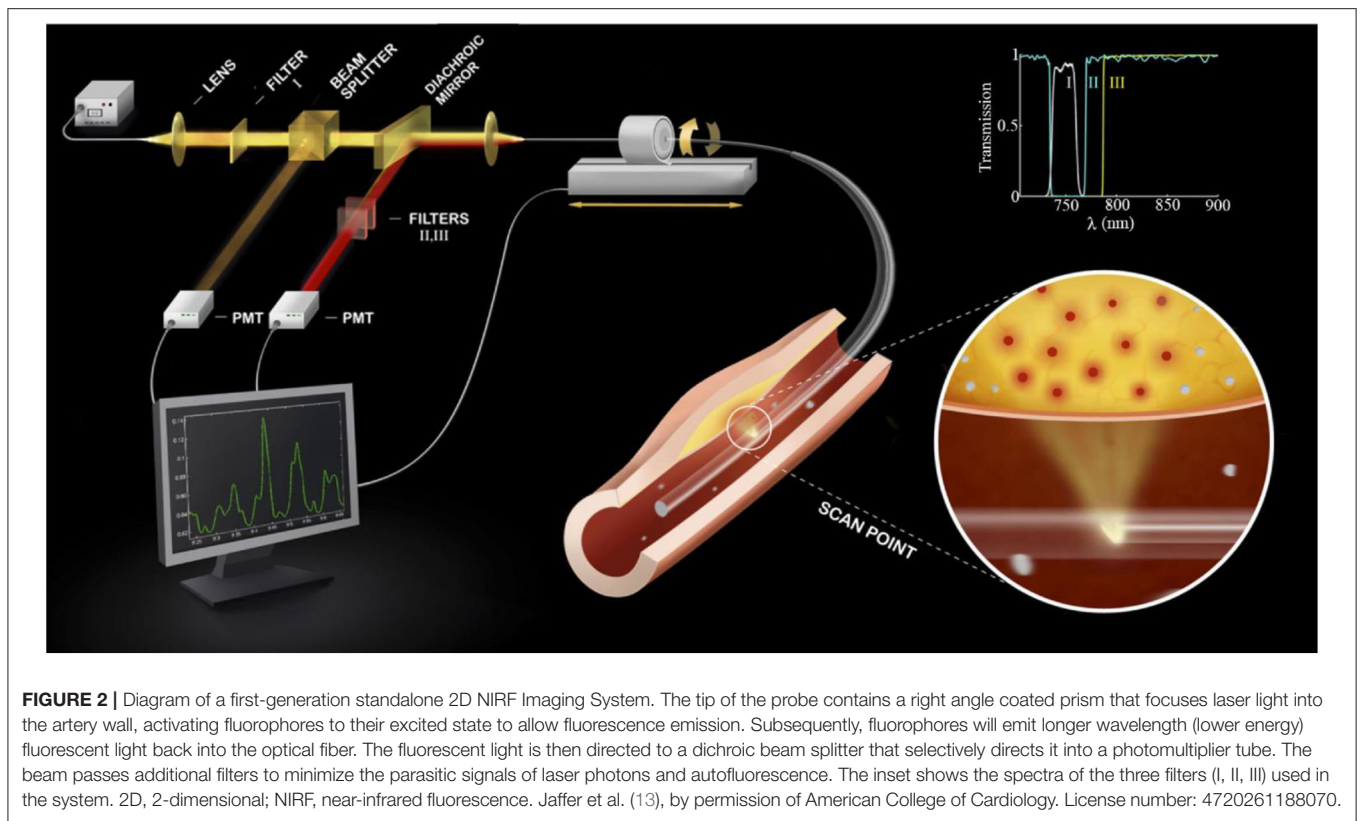
NEAR-INFRARED FLUORESCENCE (NIRF)

Basics of Near-Infrared Fluorescence (NIRF) Molecular Imaging

Near-infrared fluorescence (NIRF) is an emerging translational, intravascular imaging modality that has the ability to capture

a wide range of *in vivo* pathobiological processes (34). NIRF molecular imaging entails (1) injecting targeted or activatable NIRF molecular imaging agents, which consist of fluorescent conjugates (e.g., NIR fluorophores conjugated to an antibody, peptide, or small molecule) that concentrate in atheroma and bind to molecular targets, and (2) detecting the fluorophore emission signal from a NIRF catheter and console detection system (35). After injecting targeted fluorophores, excitation light from the near-infrared spectrum (650–900 nm) is directed at the arterial wall and used to stimulate fluorophores from ground state (S_0) to an excited state (S_1 , S_2). The excited fluorophores (S_1 , S_2) emit energy in the form of photons (fluorescence emission) and then return to the ground state, and are then available for further excitation. Fluorescence emission occurs at a lower energy and a longer wavelength, and this emission light is detectable with a high sensitivity charge-coupled device (CCD) camera and appropriate emission filter that attenuates the initial shorter wavelength excitation light (34). Compared to visible light range fluorescence detection, characteristics of NIRF imaging that make it a highly sensitive imaging modality include: (A) less light absorption by hemoglobin, lipid, and water, allowing deeper penetration of light into tissue; and (B) reduced background tissue autofluorescence, allowing for high signal-to-background ratio (36, 37).

In 2008, Jaffer et al. (38) described the first intravascular, real-time NIRF catheter-based spectroscopic



sensing probe (Figure 2). After intravenous injection of ProSense750/VM110, a cathepsin protease-activatable NIRF agent, it was possible to detect *in vivo* plaque inflammation in rabbit iliac arteries (1.5–2.5 mm in diameter) through blood (38). This system was able to detect NIRF signal in spectroscopic-type mode from a limited section of the circumferential arterial wall, given its non-rotational nature. As a result, in 2011 our group developed a two-dimensional rotational NIRF intravascular catheter with automated pullback, providing real-time, *in vivo* spatial mapping of arterial inflammation in atherosclerosis and in stented rabbit aortas (13). It is noteworthy that molecular and anatomical intravascular imaging provide complementary information about plaque structure and biology. This motivated the development of multimodal NIRF hybrid catheter systems that combines NIRF with either OCT or IVUS, for both molecular-structural co-registration, and improved quantification of NIR fluorescence signals.

NIRF Molecular Imaging Agents for Atheroma Targets

A number of NIRF molecular imaging fluorophores that target different molecular processes are now available. Those processes include protease activity, oxidized LDL, endothelial permeability, fibrin deposition, and microcalcifications. Neovascularization can be potentially detected using $\alpha v \beta 3$ integrin (39); however, to date it has not been studied for atheroma detection using intravascular NIRF catheters. At present, indocyanine green

(ICG) is the only fluorophore approved by the US Food and Drug Administration (FDA) for use in human subjects, although a number of fluorophores are undergoing FDA approval in the oncology domain (40–43) and are expected to be translated to the field of atherosclerotic cardiovascular disease (CVD).

Inflammatory Protease Activity

Atheroma macrophage inflammatory activity can be detected using protease-activatable NIR fluorophores. Cathepsins and matrix metalloproteinases (MMP) are amongst the most widely studied proteases. Cysteine cathepsins are mainly found in lysosomes and have been implicated in atheroma-blood vessel remodeling through elastolytic and collagenolytic activity (44–46). ProSense/VM110 is a cathepsin-activatable fluorophore that has been validated in animal models of atherosclerosis, and very recently has been evaluated in a patient (47). Once injected, baseline quenched ProSense/VM110 localizes to atheroma macrophages, where it is cleaved by cathepsins, yielding NIR fluorescent fragments (48). Two NIR versions of ProSense exist: ProSense 680, which is activated by Cathepsin B, L, and S with peak excitation of 680 nm and peak emission of 700 nm, and ProSense 750/VM110, activated by Cathepsins B, L, S, K, V, and D with peak excitation of 750 nm and peak emission of 780 nm (48). MMPs are another group of proteases that have been implicated in plaque destabilization (49). Similar to ProSense, gelatinases (GelSense680 and MMPsense680) are MMP-activatable fluorophores that exhibit a mosaic distribution of NIRF signal, differentiating hot spots, which correlate with

plaque instability (50, 51). Although label-free OCT detection of macrophages is possible (52, 53), NIRF offers a unique capability to visualize macrophage inflammatory activity *in vivo* is NIRF. A limitation is the need to inject ProSense/VM110 24 h prior to intended imaging; new inflammation sensors with faster pharmacokinetics are needed.

Oxidized Low-Density Lipoprotein

Oxidized LDL (oxLDL) particles are often found within atheroma lipid-rich necrotic core and have been explored as targets for NIRF imaging. Khamis et al. (11) designed a oxidized LDL NIRF targeted molecular imaging agent, termed LO1-750, that binds to oxLDL and fluoresces when illuminated with 750 nm light. LO1-750 has two components: LO1, which is an autoantibody that binds to oxidized LDL in mice, rabbits and humans (54), and AF750, which is a NIRF dye. By utilizing fluorescence molecular tomography (FMT) combined with micro-computed tomography (CT), the group showed LO1-750 accumulation within the aortic arch and its branches in atherosclerotic Ldlr^{-/-} mice when compared to wild type (WT) (11). LO1-750 generated higher NIRF signal when compared to MMP5Sense signal. *Ex vivo* imaging of rabbit aortas using intravascular NIRF catheter, showed localization of LO1-750 in atheroma lesions. This agent represents a translatable platform for future use in human subjects to enable quantifying plaque oxidative stress. A limitation for LO1-750 long circulating half-life (21 h) and wide area of distribution to the liver, kidneys, and spleen, limiting the plaque target-to-background ratio (11).

Inflammation Determined by Impaired Endothelial Permeability

Plaques that demonstrate impaired endothelial permeability are prone to erosion and thrombosis. Utilizing iron oxide nanoparticles (CLIO), Stein-Merlob et al. (55) developed a NIRF fluorophore, called CLIO-CyAm7 that was used to investigate *in vivo* endothelial dysfunction-based inflammation in a rabbit model. The group demonstrated that within atheroma plaque, CLIO-CyAm7 deposited in macrophages and endothelial cells in areas of impaired endothelial barrier underlying areas of triggered plaque thrombosis (Figure 3) (55). This insight links surface inflammation and endothelial permeability to plaque rupture *in vivo*. A limitation of this approach is the use of a long circulating nanoparticle, which may limit point-of-care applications in the cath lab.

Fibrin Deposition

Subclinical plaque rupture may result in fibrin deposition at the plaque surface. In addition, unhealed stents are characterized by fibrin deposition and absent endothelium, and are at increased risk of stent thrombosis (56). In 2012, Hara et al. (10) developed FTP11-Cy7, a fibrin-targeted peptide (FTP11), conjugated to a NIRF dye (Cy7). FTP11-Cy7 binding to fibrin was validated *in vitro* using human plasma clots and *in vivo* by binding to murine thrombi using non-invasive NIRF imaging (10). Subsequently, using rabbit model and hybrid NIRF-OCT intravascular imaging, our group was able to demonstrate that drug eluting stents (DES) showed increased fibrin deposition and fibrin persistence when compared to bare metal stents (BMS), both at day 7 and day 28 (57). This finding also revealed the limitations of standalone OCT imaging, which cannot distinguish between healthy endothelial cell coverage vs. impaired healing demarcated by fibrin deposition. Indeed, a considerable percentage of stent struts appeared covered on OCT; however, a substantial portion of OCT covered struts were in fact covered by NIRF+ fibrin, rather than re-endothelialization, and therefore may indicate an increased risk of thrombosis. A possible limitation is NIRF imaging is not possible beneath the metallic stent struts.

Microcalcifications

Similar to the process of bone formation, plaque calcification is a tightly regulated process of mineralization through the differentiation of VSMCs into osteoblasts that express osteogenic regulating proteins such as alkaline phosphatase, osteopontin, osteocalcin, osteonectin and collagen types I and II (58). When microcalcifications arise within the fibrous cap, local stress increases by 2-fold, contributing to plaque vulnerability (25). A seminal NIRF imaging study in mice demonstrated the ability to detect osteogenic activity, which precedes bulk calcification, in calcifying murine aortic valves (59). Vulnerable plaques are characterized by microcalcifications and osteogenic activity, both of which are associated with macrophage burden. OsteoSense750 (excitation 750 nm) is a NIRF agent that is derived from bisphosphonate and binds to sites of calcification *in vivo*, highlighting osteoblastic activity, and hence, potential target for vulnerability (58, 60–62). Microcalcifications can be detected by OCT; however, OCT has difficulty in visualizing cellular-level calcifications. Also NIRF has the ability to visualize osteoblastic activity (63). Only a limited studies are available on the use of OsteoSense in vascular biology and plaque vulnerability (59).

TABLE 1 | Individual and hybrid intravascular imaging in terms of detecting high risk plaque features.

	NIRF	OCT	IVUS	NIRF-OCT	NIRF-IVUS	NIRF-OCT-IVUS
Thin fibrous cap <65 μm	-	++	-	++	-	++
Lipid core	+++ (LO1-750)	+++	+	+++	+++	+++
Microcalcifications	+++ (OsteoSense)	+	+	+++	+++	+++
Macrophage infiltration	+++ (ProSense, LUM015, MMP5Sense, and GelSense and ICG)	++	-	+++	+++	+++
Neovascularization	+Bevacizumab-IR800, Integrisense	+	-	++	+	++
Remodeling	-	-	++	-	++	++

IVUS, intravenous ultrasound; NIRF, near-infrared fluorescence; OCT, optical coherence tomography.

HYBRID INTRAVASCULAR NEAR-INFRARED FLUORESCENCE MOLECULAR IMAGING

Standalone NIRF imaging does not allow for distance correction and localization of the source of NIR light excitation and fluorescence emission. In addition, separate NIRF catheter-based imaging and then structural based imaging (e.g., IVUS, OCT) is impractical for clinical use. For these reasons, hybrid intravascular molecular-structural catheters have been developed to enable concurrent co-registration of molecular and anatomical images, and accurate distance-based correction/quantification of the NIRF signal (Tables 1, 2) (64, 66).

Hybrid NIRF-OCT

OCT generates images with high spatial resolution (10–20 μm) but with relatively low depth of penetration (1–2 mm) (65). When combined with NIRF, the resulting hybrid catheter provides complementary data on plaque structure and biology (Figure 4). Two hybrid NIRF-OCT catheters have been developed; due to the OCT component, saline/contrast flushing is required during imaging acquisition. In 2011, Yoo et al. (66) developed a dual modality NIRF-OCT rotary catheter system with automated pullback and probe size of 2.4 Fr. The imaging probe comprised of a double-clad fiber with a single mode OCT core (1,320 nm) and inner cladding for NIR fluorescence collection (66). The system was validated using cadaveric human coronary artery with an implanted NIRF-fibrin labeled stent, and *in vivo* rabbit iliac arteries after balloon injury (66). Similarly, Lee et al. (68) designed a 2.6 Fr NIRF-OCT probe with frame acquisition rate of 100/s compared to 25.4/s in the Yoo et al. first-generation system. Using atherosclerosis rabbit models, ICG deposition was reliably identified in lipid- and macrophage-rich plaques *in vivo* (68). Later, the same group validated the use of NIRF-OCT system in drug eluting stent (DES)-stented swine coronary arteries, showing ICG localization within atheroma and behind implanted DES (69). Since NIRF-OCT is an all-optical fiber-based system, the engineering of the probe is more straightforward, compared to NIRF-IVUS or NIRF-IVUS-photoacoustic systems. Limitations of this system are low depth of penetration, and the need to flush during OCT image acquisition.

Hybrid NIRF-IVUS

IVUS was introduced to clinical practice in early 1990s (70), and ever since has been the most widely used intravascular imaging modality due to decent depth of penetration (5–8 mm) and moderate backscatter from blood between 20 and 50 MHz (does not require blood clearance), with a limitation of intermediate spatial resolution (100–250 μm) (65). Dixon and Hossack (71) designed the first NIRF-IVUS hybrid probe and validated its use in phantom coronary arteries. One limitation of this system was the relatively larger probe size of 4.2 Fr due to side-by-side probe arrangement, precluding its use in typical diameter coronary arteries. Subsequently, Abran et al. (64, 72) developed a similar NIRF-IVUS bimodal catheter, and assessed its validity using ICG in *ex vivo* rabbit atherosclerosis model. The first *in vivo*

TABLE 2 | Characteristics of NIRF hybrid intravascular molecular imaging.

	Probe diameter	Fiber characteristics	Depth of penetration	Axial resolution	Frame rate	Limitation
NIRF-OCT	2.4 Fr	<ul style="list-style-type: none"> OCT: 1,320 nm NIRF: 750 nm 	NIRF: 3 mm	OCT: 7 μm	25.4/s	Slower image acquisition speed
	2.6 Fr	<ul style="list-style-type: none"> OCT: 1,290 nm NIRF: 749–790 nm 	OCT: 1–2 mm	OCT: 7 μm	100/s	–
NIRF-IVUS	4.2 Fr	<ul style="list-style-type: none"> IVUS: 45 MHz NIRF: 750 nm 	<ul style="list-style-type: none"> IVUS: 4 mm NIRF: 2 mm 	IVUS: N/A	30/s	Large probe size
	4.5 Fr	<ul style="list-style-type: none"> IVUS: 40 MHz NIRF: 750 nm 	<ul style="list-style-type: none"> IVUS: 4 mm NIRF: 2 mm 	IVUS: 150 μm	2.7/s	Large probe size
	9.0 Fr	<ul style="list-style-type: none"> IVUS: 15 MHz NIRF: 750 nm 	<ul style="list-style-type: none"> IVUS: 4 mm NIRF: 2 mm 	IVUS: 270 μm	2.7/s	Large probe size
NIRF-IVUS-OCT	3.9 Fr	<ul style="list-style-type: none"> OCT: 1,310 nm NIRF: 785 nm IVUS: 40 MHz 	<ul style="list-style-type: none"> OCT: 3–5 mm IVUS: 5–6 mm NIRF: 3–5 mm 	–	20/s	Large probe size

IVUS, intravenous ultrasound; NIRF, near-infrared fluorescence; OCT, optical coherence tomography.

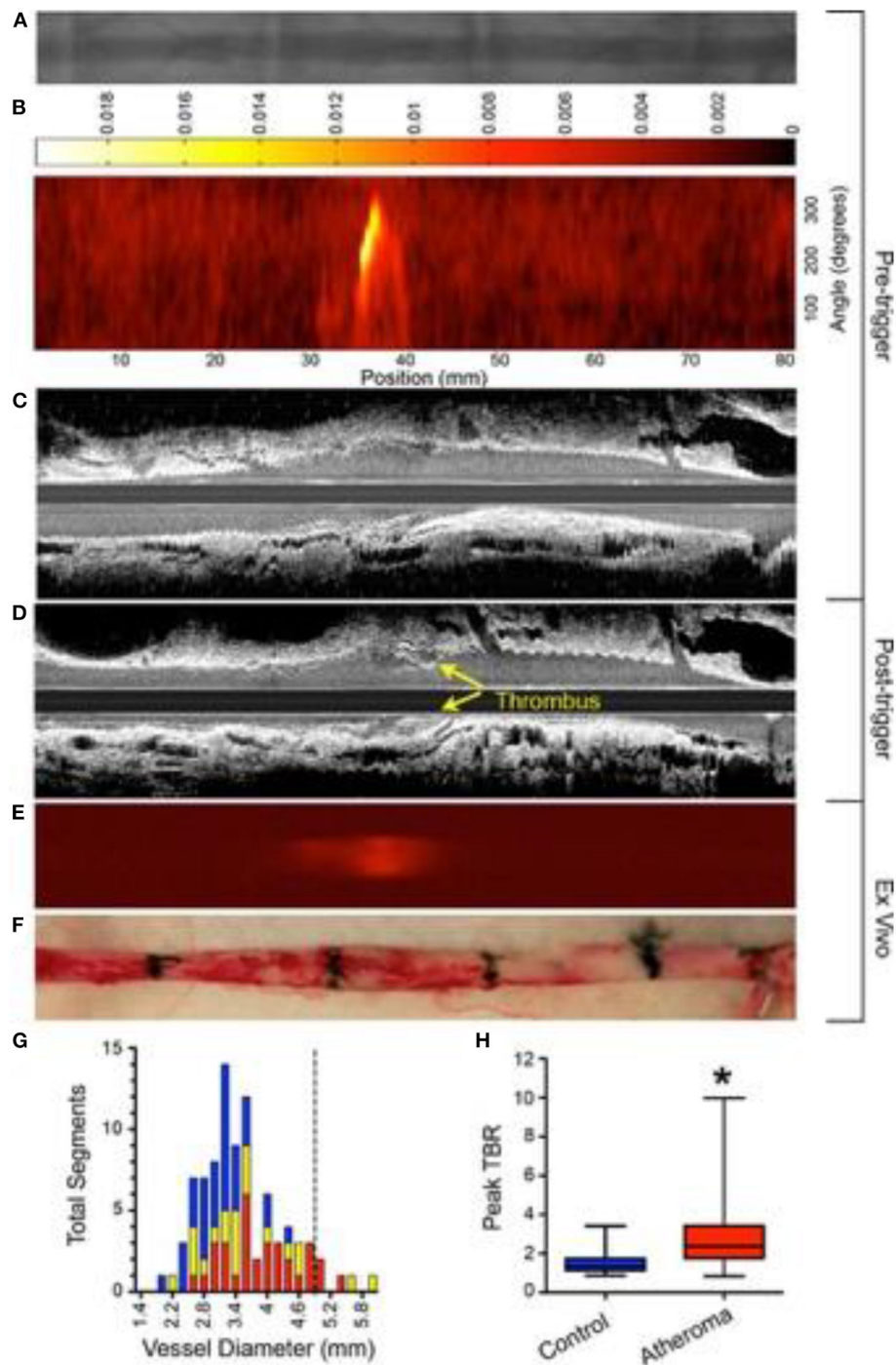
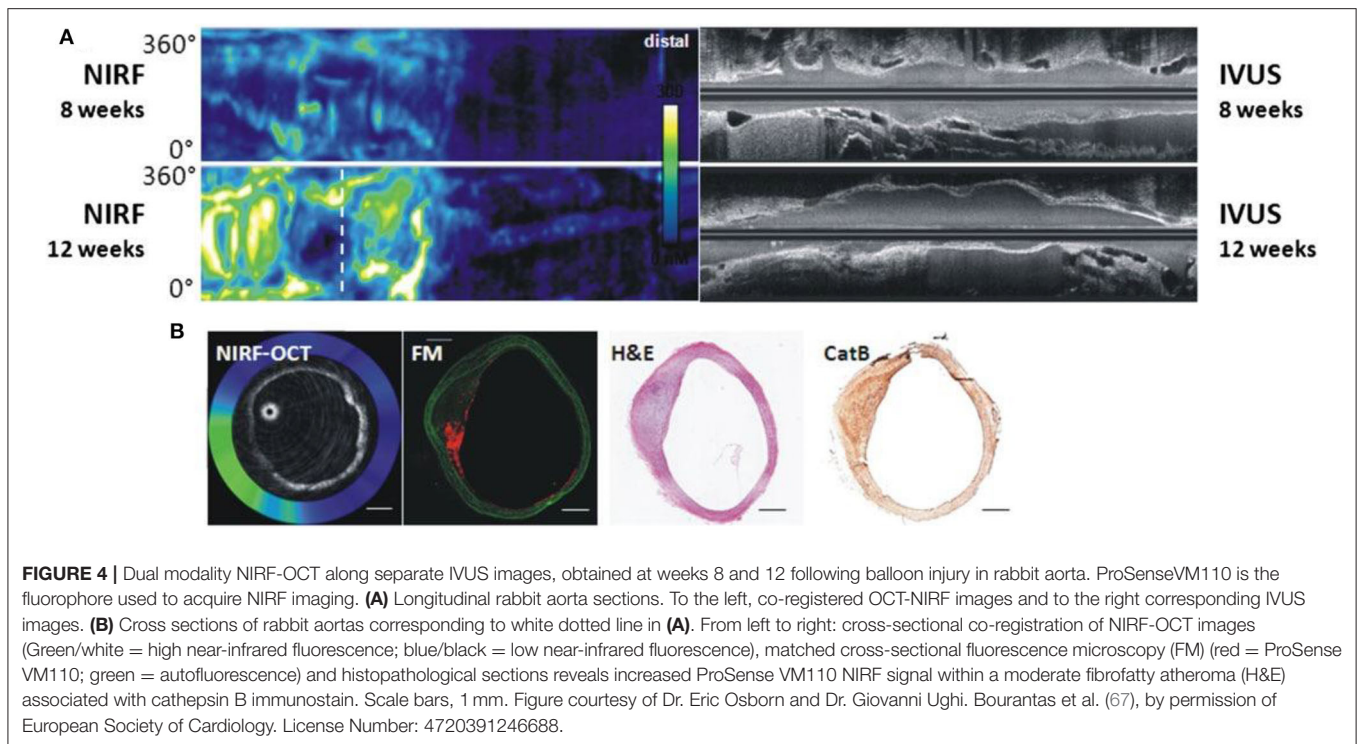


FIGURE 3 | Experimental *in vivo* and *ex vivo* near-infrared fluorescence (NIRF) imaging of inflammation and subsequent atherothrombosis. Rabbits underwent balloon injury at week 2, and were fed high cholesterol diet till week 8. Ten weeks after balloon injury, rabbits received CLIO-CyAm7 (a inflammation-sensitive nanoparticle-based fluorophore), and underwent pharmacologic-triggered plaque thrombosis 24 h later. **(A)** Pre-trigger x-ray angiography showing the aorta for image coregistration. **(B)** Pre-trigger *in vivo* NIRF imaging projected into a 2-dimensional (2D) matrix showing an area of increased signal between 30 and 40 mm. **(C,D)** Pre- and post-trigger intravascular ultrasound (IVUS) imaging demonstrating induced luminal thrombus (yellow arrows) corresponding to the region of increased NIRF signal intensity on pretrigger NIRF imaging in **(B)**. **(E,F)** *Ex vivo* fluorescence reflectance imaging of cross-linked iron oxide (CLIO)-CyAm7 verifying *in vivo* 2D NIRF imaging, and gross pathology of the resected aorta with 1.5 cm black tissue markings for histological analysis and coregistration. **(G)** Histogram of vessel diameter measured by cross-sectional IVUS imaging. Red indicates atheroma without attached thrombus, yellow indicates atheroma with attached thrombus, and blue indicates uninjured control aortic segments. The dashed line indicates the 5 mm cut-off for exclusion of NIRF imaging data because of distance attenuation of the NIRF signal in large vessels. **(H)** *In vivo* 2D NIRF imaging revealed significantly higher target/background ratio (TBR) in areas with atheroma, compared with uninjured segments of the aorta (peak TBR 2.86 ± 1.82 and 1.55 ± 0.65 , $*P = 0.001$). Stein-Merlob et al. (55), by permission of American Heart Association (AHA). License number: 4720560395030.



validation of a bimodal NIRF-IVUS system was demonstrated by Bozhko et al. (73) in angioplasty-induced vascular injury in swine peripheral arteries and experimental fibrin deposition on coronary artery stents, and of atheroma in a rabbit aorta, using ICG. Clinical translation of this hybrid catheter necessitates designing a smaller probe <3.0 Fr, appropriate for intracoronary use, and will likely require re-engineering of side-by-side designs to serial designs, similar to current clinical IVUS-NIR spectroscopy catheters.

Hybrid trimodal NIRF-OCT-IVUS Catheter

A tri-hybrid intravascular probe using IVUS, OCT and NIRF technologies was developed by Li et al. (74), offering the potential for multi-structural and molecular imaging in a single pullback. The system was validated using phantom and *ex vivo* experiments using pig and rabbit arteries (74). While this system offers the advantages of the three imaging modalities combined, the probe size at present (3.9 Fr) is currently too large for routine clinical type applications, but is an exciting advance nonetheless, and we await further validation *in vivo*.

NIRAF-OCT IMAGING

While NIRF intracoronary molecular imaging has not been performed in human subjects, a recent advance was the demonstration of clinical intracoronary OCT-NIR-autofluorescence (NIRAF, based at 633 nm), a new contrast-free autofluorescence-based method (75). In the first human study on 12 patients with CAD undergoing PCI, Ughi et al. (75) demonstrated that NIRAF signal correlated with vulnerable

features like fibroatheroma, plaque rupture and in-stent restenosis in non-culprit lesions (75). Additionally, NIRAF signal was associated with components of components of intraplaque hemorrhage (e.g., bilirubin, protoporphyrin IX) (76). While NIRAF molecular imaging is very promising intravascular imaging modality, the complete set of molecules and biological processes underlying NIRAF remain to be elucidated. Compared to NIRAF, NIRF imaging through molecular-specific imaging agents allows targeting of specific patho-biological processes, like protease activity, oxidized LDL, endothelial permeability, fibrin deposition, and osteogenesis.

PHOTOACOUSTIC IMAGING

Intravascular photoacoustic (IVPA) is an emerging imaging modality that is a natural extension of IVUS, and has the potential to detect certain fluorophores and nanomaterials that could enable IVPA-based molecular imaging. IVPA is a novel structural and molecular imaging modality that uses multiple wavelengths to illuminate the tissue of interest and identifies the acoustic waves generated by the thermoelastic expansion of the environment surrounding absorbing molecules (77). In an *in vivo* experiment on rabbit aortas, Wang et al. (78) showed that IVPA/IVUS imaging can identify lipid deposits within vessel wall through the blood without the need of saline flushing or balloon occlusion. Excitingly, IVPA provided 3 dimensional images of the vessel wall. Recently, Iskandder-Risk et al. demonstrated IVPA *in vivo* imaging of swine coronary artery. The quality of images were adjudicated using OCT and histology (79).

TRANSLATIONAL OUTLOOK

To enable clinical intracoronary NIRF molecular imaging, the NIRF system will need to switch to 750–800 nm excitation, and clinical targeted/activatable NIRF imaging agents will need to be available. Currently, indocyanine green (ICG, ex/em 805/830 nm) is the only atherosclerosis-targeted NIR fluorophore approved by the US Food and Drug Administration (FDA) for human use, facilitating the use of NIRF catheter in human subjects once approved. The recognition that ICG, a blood flow imaging agent available for 50 years, could target atherosclerosis was somewhat unexpected. In 2011, Vinegoni et al. recognized that the amphiphilic properties of ICG

might allow it to have an atheroma targeting profile. Using intravascular and *ex vivo* NIRF imaging, ICG was found to accumulate in atheroma macrophages and was detected *in vivo* rabbit atheroma (80), and in pig coronary plaques (69, 81). Subsequently in 2016, The BRIGHT-CEA trial (Indocyanine Green Fluorescence Uptake in Human Carotid Artery Plaque, a study of injection of ICG prior to patients undergoing carotid endarterectomy) was conducted (81). Five patients undergoing carotid endarterectomy were injected with ICG; plaques were resected 99 min afterwards. *Ex vivo* intravascular NIRF-OCT and fluorescence reflectance imaging showed that ICG NIRF signal localized to and accumulated in human atheroma for the first time in living patients (Figure 5). The authors concluded that

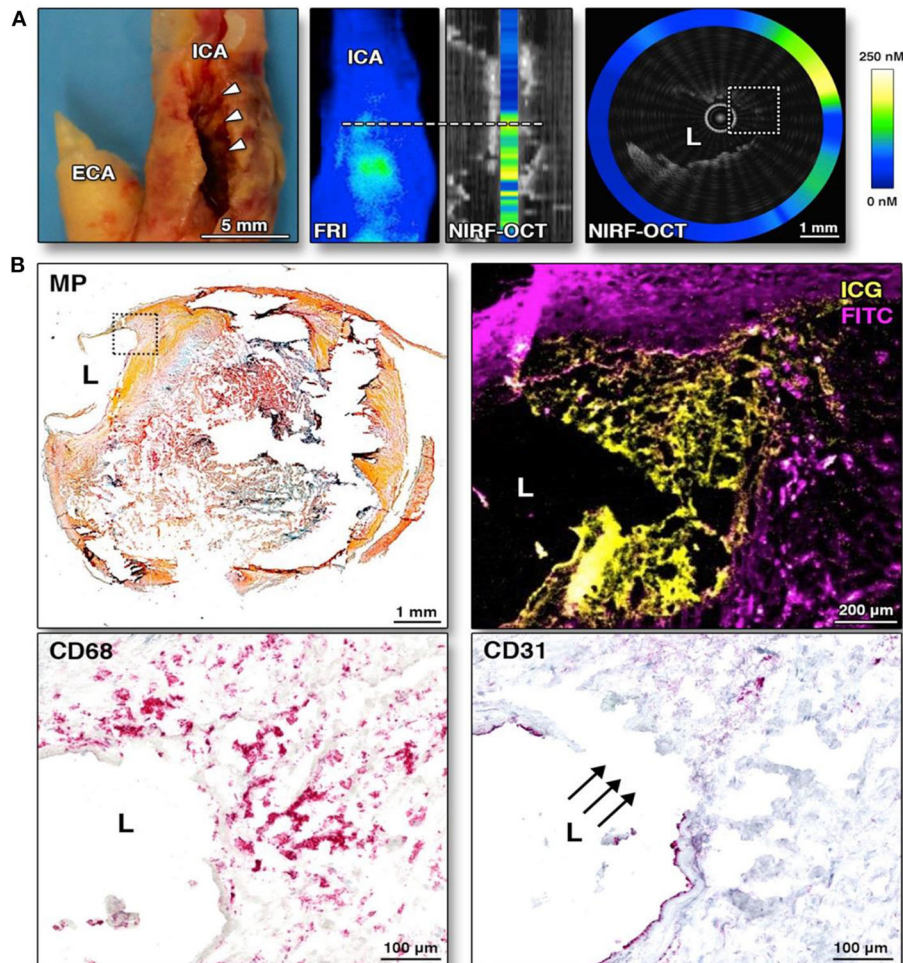
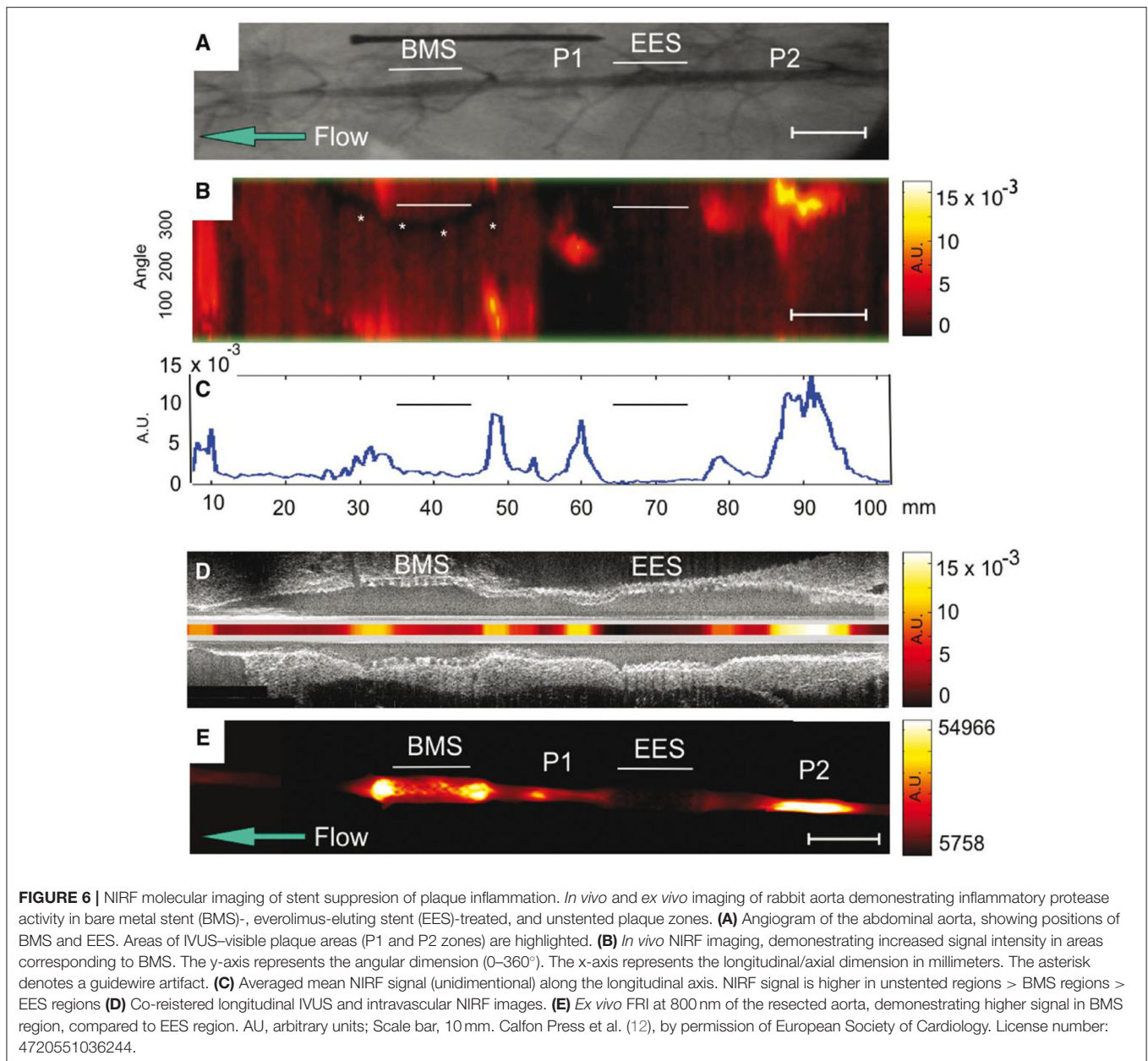


FIGURE 5 | *Ex-vivo* intravascular NIRF-OCT images of human carotid arteries following ICG injection and then endarterectomy. ICG was injected into human subjects 99 min prior to endarterectomy. ICG accumulates in atherosclerotic area especially endothelial discontinuation. **(A)** Corresponding gross internal carotid artery (ICA) specimen, along with corresponding fluorescence reflectance image (FRI), and NIRF-OCT cross sectional, coregistered images, illustrating similar ICG uptake pattern (light blue = low ICG signal; green-yellow = high ICG signal) at the stenotic region (white arrowheads) in the ICA. **(B)** Histological analysis of the same area of the NIRF-OCT cross-sectional image shown in **(A)**. Movat pentachrome (MP) shows a complex atherosclerotic plaque with a large necrotic core with lipid and cellular infiltration (dotted box). Higher magnification (10×) fluorescence microscopy of the boxed area illustrates ICG NIRF signal adjacent to the lumen, which is distinct from fluorescein isothiocyanate (FITC)-channel autofluorescence. CD68 staining of the same area validates that the ICG NIRF signal (yellow pseudocolor) spatially relates to CD68-defined plaque macrophages beneath the area of intimal disruption. The disruption is confirmed by CD31 staining in this same area. ECA, external carotid artery. Verjans et al. (81), by permission of American College of Cardiology (ACC). License number: 4720551416574.



ICG accumulated in plaques with impaired endothelial integrity, disrupted fibrous cap, and area of neovascularization (81). This study may pave the way for future human intracoronary NIRF-OCT using ICG to image pathobiological aspects of coronary atherosclerosis.

Another translatable aspect is the use of NIRF imaging to detect plaque inflammation modified by stent placement, and predict complications such as in-stent thrombosis and stenosis. Using an atheroma rabbit model, Calfon Press et al. (12) showed that everolimus-eluting DES could decrease *in vivo* plaque inflammation and macrophage accumulation. This finding provides evidence that DES may be a bio-stabilizer of high-risk, inflamed plaques (Figure 6), although neoatherosclerosis is still a

potential limitation of such approach. In a recent study, Osborn et al. (82) have demonstrated that plaque inflammation is an independent predictor of plaque progression, using atheroma rabbit model and serial NIRF-OCT. These preclinical studies will provide an outline for clinical studies once a NIRF catheter is approved.

CONCLUSION AND FUTURE DIRECTIONS

Intravascular NIRF molecular imaging offers a new dimension for plaque assessment based on pathobiology, a key driver of coronary events, and is on the verge of clinical translation to human coronary arteries. We envision that intravascular

NIRF-OCT or NIRF-IVUS molecular-structural imaging will be used to comprehensively assess the coronary artery of patients already undergoing percutaneous coronary intervention. As PCI is now routinely being performed with intravascular imaging (IVUS or OCT), we anticipate that the only difference for NIRF-OCT or NIRF-IVUS will be the administration of a targeted molecular imaging agent at the start of PCI. Following PCI, completion NIRF-OCT or NIRF-IVUS will be performed, allowing assessment of non-culprit coronary artery segments proximal and distal to the target lesion that was stented. This will allow the generation of an integrated molecular-structural atheroma score reflecting the degree of pathobiology for the culprit artery. In addition another artery could be potentially imaged with the same goal. Ultimately, a NIRF-based pathobiology score will identify high-risk lesions, arteries, and patients, allowing the ability to more precisely target newer

atheroma medical therapies (e.g., PCSK9 inhibitors, icosapent ethyl, ezetimibe, GLP1-receptor antagonists, SGLT2 inhibitors) to those at highest risk. Overall, integration of NIRF pathobiology assessment will enable personalized medical therapy for patients with CAD, instead of a one size fits all approach as currently practiced worldwide (e.g., statin and dual anti-platelet therapy, regardless of underlying pathobiological risk).

AUTHOR CONTRIBUTIONS

Both authors contributed to the writing of this review article.

FUNDING

This work was supported by NIH 1R01HL137913 (FAJ) and 1R01HL150538 (FAJ)

REFERENCES

- Muller JE, Tofler GH, Stone PH. Circadian variation and triggers of onset of acute cardiovascular disease. *Circulation*. (1989) 79:733–43. doi: 10.1161/01.CIR.79.4.733
- Schaar JA, Muller JE, Falk E, Virmani R, Fuster V, Serruys PW, et al. Terminology for high-risk and vulnerable coronary artery plaques. Report of a meeting on the vulnerable plaque, June 17 and 18, 2003, Santorini, Greece. *Eur Heart J*. (2004) 25:1077–82. doi: 10.1016/j.ehj.2004.01.002
- Narula J, Nakano M, Virmani R, Kolodgie FD, Petersen R, Newcomb R, et al. Histopathologic characteristics of atherosclerotic coronary disease and implications of the findings for the invasive and noninvasive detection of vulnerable plaques. *J Am Coll Cardiol*. (2013) 61:1041–51. doi: 10.1016/j.jacc.2012.10.054
- Burke AP, Farb A, Malcom GT, Liang YH, Smialek J, Virmani R. Coronary risk factors and plaque morphology in men with coronary disease who died suddenly. *N Engl J Med*. (1997) 336:1276–82. doi: 10.1056/NEJM199705013361802
- van der Wal AC, Becker AE, van der Loos CM, Das PK. Site of intimal rupture or erosion of thrombosed coronary atherosclerotic plaques is characterized by an inflammatory process irrespective of the dominant plaque morphology. *Circulation*. (1994) 89:36–44. doi: 10.1161/01.CIR.89.1.36
- Bode MF, Jaffer FA. IVUS and OCT: Current state-of-the-art in intravascular coronary imaging. *Curr Cardiovasc Imaging Rep*. (2019) 12:29. doi: 10.1007/s12410-019-9503-7
- Stone PH, Saito S, Takahashi S, Makita Y, Nakamura S, Kawasaki T, et al. Prediction of progression of coronary artery disease and clinical outcomes using vascular profiling of endothelial shear stress and arterial plaque characteristics: the PREDICTION study. *Circulation*. (2012) 126:172–81. doi: 10.1161/CIRCULATIONAHA.112.096438
- Xie Y, Mintz GS, Yang J, Doi H, Iñiguez A, Dangas GD, et al. Clinical outcome of nonculprit plaque ruptures in patients with acute coronary syndrome in the PROSPECT study. *JACC Cardiovasc Imaging*. (2014) 7:397–405. doi: 10.1016/j.jcmg.2013.10.010
- Stone GW, Maehara A, Lansky AJ, de Bruyne B, Cristea E, Mintz GS, et al. A prospective natural-history study of coronary atherosclerosis. *N Engl J Med*. (2011) 364:226–35. doi: 10.1056/NEJMoa1002358
- Hara T, Bhayana B, Thompson B, Kessinger CW, Khatri A, McCarthy JR, et al. Molecular imaging of fibrin deposition in deep vein thrombosis using fibrin-targeted near-infrared fluorescence. *JACC Cardiovasc Imaging*. (2012) 5:607–15. doi: 10.1016/j.jcmg.2012.01.017
- Khamis RY, Woollard KJ, Hyde GD, Boyle JJ, Bicknell C, Chang S-H, et al. Near Infrared Fluorescence (NIRF) molecular imaging of oxidized LDL with an autoantibody in experimental atherosclerosis. *Sci Rep*. (2016) 6:21785. doi: 10.1038/srep21785
- Calfon Press MA, Mallas G, Rosenthal A, Hara T, Mauskapf A, Nudelman RN, et al. Everolimus-eluting stents stabilize plaque inflammation *in vivo*: assessment by intravascular fluorescence molecular imaging. *Eur Heart J Cardiovasc Imaging*. (2017) 18:510–18. doi: 10.1093/ehjci/jew228
- Jaffer FA, Calfon MA, Rosenthal A, Mallas G, Razansky RN, Mauskapf A, et al. Two-dimensional intravascular near-infrared fluorescence molecular imaging of inflammation in atherosclerosis and stent-induced vascular injury. *J Am Coll Cardiol*. (2011) 57:2516–26. doi: 10.1016/j.jacc.2011.02.036
- Wu M-Y, Li C-J, Hou M-F, Chu P-Y. New insights into the role of inflammation in the pathogenesis of atherosclerosis. *Int J Mol Sci*. (2017) 18:2034. doi: 10.3390/ijms18102034
- Khalil MF, Wagner WD, Goldberg IJ. Molecular interactions leading to lipoprotein retention and the initiation of atherosclerosis. *Arterioscler Thromb Vasc Biol*. (2004) 24:2211–8. doi: 10.1161/01.ATV.0000147163.54024.70
- Williams KJ. Arterial wall chondroitin sulfate proteoglycans: diverse molecules with distinct roles in lipoprotein retention and atherogenesis. *Curr Opin Lipidol*. (2001) 12:477–87. doi: 10.1097/00041433-200110000-00002
- Bentzon JE, Otsuka F, Virmani R, Falk E. Mechanisms of plaque formation and rupture. *Circ Res*. (2014) 114:1852–66. doi: 10.1161/CIRCRESAHA.114.302721
- Bom MJ, van der Heijden DJ, Kedhi E, van der Heyden J, Meuwissen M, Knaapen P, et al. Early detection and treatment of the vulnerable coronary plaque: can we prevent acute coronary syndromes? *Circ Cardiovasc Imaging*. (2017) 10:e005973. doi: 10.1161/CIRCIMAGING.116.005973
- Zhou M-S, Chadipiralla K, Mendez AJ, Jaimes EA, Silverstein RL, Webster K, et al. Nicotine potentiates proatherogenic effects of oxLDL by stimulating and upregulating macrophage CD36 signaling. *Am J Physiol Heart Circ Physiol*. (2013) 305:H563–74. doi: 10.1152/ajpheart.00042.2013
- Falk E. Pathogenesis of atherosclerosis. *J Am Coll Cardiol*. (2006) 47:C7–12. doi: 10.1016/j.jacc.2005.09.068
- Bennett MR, Sinha S, Owens GK. Vascular smooth muscle cells in atherosclerosis. *Circ Res*. (2016) 118:692–702. doi: 10.1161/CIRCRESAHA.115.306361
- Yahagi K, Kolodgie FD, Otsuka F, Finn AV, Davis HR, Joner M, et al. Pathophysiology of native coronary, vein graft, and in-stent atherosclerosis. *Nat Rev Cardiol*. (2016) 13:79–98. doi: 10.1038/nrcardio.2015.164
- New SEP, Aikawa E. Role of extracellular vesicles in *de novo* mineralization: an additional novel mechanism of cardiovascular calcification. *Arterioscler Thromb Vasc Biol*. (2013) 33:1753–8. doi: 10.1161/ATVBAHA.112.300128
- Nakahara T, Dweck MR, Narula N, Pisapia D, Narula J, Strauss HW. Coronary artery calcification: from mechanism to molecular imaging. *JACC Cardiovasc Imaging*. (2017) 10:582–93. doi: 10.1016/j.jcmg.2017.03.005
- Vengrenyuk Y, Carlier S, Xanthos S, Cardoso L, Ganatos P, Virmani R, et al. A hypothesis for vulnerable plaque rupture due to stress-induced debonding around cellular microcalcifications in thin fibrous caps. *Proc Natl Acad Sci USA*. (2006) 103:14678–83. doi: 10.1073/pnas.0606310103

26. Milzi A, Burgmaier M, Burgmaier K, Hellmich M, Marx N, Reith S. Type 2 diabetes mellitus is associated with a lower fibrous cap thickness but has no impact on calcification morphology: an intracoronary optical coherence tomography study. *Cardiovasc Diabetol.* (2017) 16:152. doi: 10.1186/s12933-017-0635-2
27. Lee JM, Choi KH, Koo B-K, Park J, Kim J, Hwang D, et al. Prognostic implications of plaque characteristics and stenosis severity in patients with coronary artery disease. *J Am Coll Cardiol.* (2019) 73:2413–24. doi: 10.1016/j.jacc.2019.02.060
28. Narula J, Strauss HW. The popcorn plaques. *Nat Med.* (2007) 13:532–4. doi: 10.1038/nm0507-532
29. Libby P, Ridker PM, Hansson GK, Leducq Transatlantic Network on Atherothrombosis. Inflammation in atherosclerosis: from pathophysiology to practice. *J Am Coll Cardiol.* (2009) 54:2129–38. doi: 10.1016/j.jacc.2009.09.009
30. Mehta SR, Wood DA, Storey RF, Mehran R, Bainey KR, Nguyen H, et al. Complete revascularization with multivessel PCI for myocardial infarction. *N Engl J Med.* (2019) 381:1411–21. doi: 10.1056/NEJMoa1907775
31. Kubo T, Maehara A, Mintz GS, Doi H, Tsujita K, Choi S-Y, et al. The dynamic nature of coronary artery lesion morphology assessed by serial virtual histology intravascular ultrasound tissue characterization. *J Am Coll Cardiol.* (2010) 55:1590–7. doi: 10.1016/j.jacc.2009.07.078
32. Zhao Z, Witzensbichler B, Mintz GS, Jaster M, Choi S-Y, Wu X, et al. Dynamic nature of nonculprit coronary artery lesion morphology in STEMI: a serial IVUS analysis from the HORIZONS-AMI trial. *JACC Cardiovasc Imaging.* (2013) 6:86–95. doi: 10.1016/j.jcmg.2012.08.010
33. Papadopoulou S-L, Neeffes LA, Garcia-Garcia HM, Flu W-J, Rossi A, Dharampal AS, et al. Natural history of coronary atherosclerosis by multislice computed tomography. *JACC Cardiovasc Imaging.* (2012) 5:S28–37. doi: 10.1016/j.jcmg.2012.01.009
34. Calfon MA, Rosenthal A, Mallas G, Mauskapf A, Nudelman RN, Ntziachristos V, et al. *In vivo* near infrared fluorescence (NIRF) intravascular molecular imaging of inflammatory plaque, a multimodal approach to imaging of atherosclerosis. *J Vis Exp.* (2011) 54:2257. doi: 10.3791/2257
35. Chowdhury MM, Tawakol A, Jaffer FA. Molecular imaging of atherosclerosis: a clinical focus. *Curr Cardiovasc Imaging Rep.* (2017) 10:2. doi: 10.1007/s12410-017-9397-1
36. Hong G, Antaris AL, Dai H. Near-infrared fluorophores for biomedical imaging. *Nat Biomed Eng.* (2017) 1:0010. doi: 10.1038/s41551-016-0010
37. Sevick-Muraca EM, Rasmussen JC. Molecular imaging with optics: primer and case for near-infrared fluorescence techniques in personalized medicine. *J Biomed Opt.* (2008) 13:041303. doi: 10.1117/1.2953185
38. Jaffer FA, Vinegoni C, John MC, Aikawa E, Gold HK, Finn AV, et al. Real-time catheter molecular sensing of inflammation in proteolytically active atherosclerosis. *Circulation.* (2008) 118:1802–9. doi: 10.1161/CIRCULATIONAHA.108.785881
39. Lin S-A, Patel M, Suresch D, Connolly B, Bao B, Groves K, et al. Quantitative longitudinal imaging of vascular inflammation and treatment by ezetimibe in apoE mice by FMT using new optical imaging biomarkers of cathepsin activity and $\alpha(v)\beta(3)$ integrin. *Int J Mol Imaging.* (2012) 2012:189254. doi: 10.1155/2012/189254
40. van Dam GM, Themelis G, Crane LMA, Harlaar NJ, Pleijhuis RG, Kelder W, et al. Intraoperative tumor-specific fluorescence imaging in ovarian cancer by folate receptor- α targeting: first in-human results. *Nat Med.* (2011) 17:1315–19. doi: 10.1038/nm.2472
41. Whitley MJ, Cardona DM, Lazarides AL, Spasojevic I, Ferrer JM, Cahill J, et al. A mouse-human phase 1 co-clinical trial of a protease-activated fluorescent probe for imaging cancer. *Sci Transl Med.* (2016) 8:320ra4. doi: 10.1126/scitranslmed.aad0293
42. Harlaar NJ, Koller M, de Jongh SJ, van Leeuwen BL, Hemmer PH, Kruijff S, et al. Molecular fluorescence-guided surgery of peritoneal carcinomatosis of colorectal origin: a single-centre feasibility study. *Lancet Gastroenterol Hepatol.* (2016) 1:283–90. doi: 10.1016/S2468-1253(16)30082-6
43. Nagengast WB, Hartmans E, Garcia-Allende PB, Peters FTM, Linszen MD, Koch M, et al. Near-infrared fluorescence molecular endoscopy detects dysplastic oesophageal lesions using topical and systemic tracer of vascular endothelial growth factor A. *Gut.* (2019) 68:7–10. doi: 10.1136/gutjnl-2017-314953
44. Turk V, Stoka V, Vasiljeva O, Renko M, Sun T, Turk B, et al. Cysteine cathepsins: from structure, function and regulation to new frontiers. *Biochim Biophys Acta.* (2012) 1824:68–88. doi: 10.1016/j.bbapap.2011.10.002
45. Sukhova GK, Shi GP, Simon DI, Chapman HA, Libby P. Expression of the elastolytic cathepsins S and K in human atheroma and regulation of their production in smooth muscle cells. *J Clin Invest.* (1998) 102:576–83. doi: 10.1172/JCI181
46. Jaffer FA, Kim D-E, Quinti L, Tung C-H, Aikawa E, Pande AN, et al. Optical visualization of cathepsin K activity in atherosclerosis with a novel, protease-activatable fluorescence sensor. *Circulation.* (2007) 115:2292–8. doi: 10.1161/CIRCULATIONAHA.106.660340
47. *VM110 in Detection of Microscopic Tumors: A Phase I Study.* Full Text View. ClinicalTrials.gov. Available online at: <https://clinicaltrials.gov/ct2/show/NCT03286062> (accessed December 1, 2019).
48. Jaffer FA, Weissleder R. Seeing within: molecular imaging of the cardiovascular system. *Circ Res.* (2004) 94:433–45. doi: 10.1161/01.RES.0000119321.18573.5A
49. Newby AC. Metalloproteinase production from macrophages - a perfect storm leading to atherosclerotic plaque rupture and myocardial infarction. *Exp Physiol.* (2016) 101:1327–37. doi: 10.1113/EP085567
50. Wallis de Vries BM, Hillebrands J-L, van Dam GM, Tio RA, de Jong JS, Slart RHJA, et al. Images in cardiovascular medicine. Multispectral near-infrared fluorescence molecular imaging of matrix metalloproteinases in a human carotid plaque using a matrix-degrading metalloproteinase-sensitive activatable fluorescent probe. *Circulation.* (2009) 119:e534–6. doi: 10.1161/CIRCULATIONAHA.108.821389
51. Deguchi J, Aikawa M, Tung C-H, Aikawa E, Kim D-E, Ntziachristos V, et al. Inflammation in atherosclerosis: visualizing matrix metalloproteinase action in macrophages *in vivo*. *Circulation.* (2006) 114:55–62. doi: 10.1161/CIRCULATIONAHA.106.619056
52. Tearney GJ. OCT imaging of macrophages. *JACC.* (2015) 8:73–5. doi: 10.1016/j.jcmg.2014.09.019
53. Tearney GJ, Yabushita H, Houser SL, Aretz HT, Jang I-K, Schliendorf KH, et al. Quantification of macrophage content in atherosclerotic plaques by optical coherence tomography. *Circulation.* (2003) 107:113–19. doi: 10.1161/01.CIR.0000044384.41037.43
54. Chang S-H, Johns M, Boyle JJ, McConnell E, Kirkham PA, Bicknell C, et al. Model IgG monoclonal autoantibody-anti-idiotypic pair for dissecting the humoral immune response to oxidized low density lipoprotein. *Hybridoma.* (2012) 31:87–98. doi: 10.1089/hyb.2011.0058
55. Stein-Merlob AF, Hara T, McCarthy JR, Mauskapf A, Hamilton JA, Ntziachristos V, et al. Atheroma susceptible to thrombosis exhibit impaired endothelial permeability *in vivo* as assessed by nanoparticle-based fluorescence molecular imaging. *Circ Cardiovasc Imaging.* (2017) 10:e005813. doi: 10.1161/CIRCIMAGING.116.005813
56. Finn AV, JM, Nakazawa G, KF, Newell JMC. Pathological correlates of late drug-eluting stent thrombosis: strut coverage as a marker of endothelialization. *Circulation.* (2007) 115:2435–41. doi: 10.1161/CIRCULATIONAHA.107.693739
57. Hara T, Ughi GJ, McCarthy JR, Erdem SS, Mauskapf A, Lyon SC, et al. Intravascular fibrin molecular imaging improves the detection of unhealed stents assessed by optical coherence tomography *in vivo*. *Eur Heart J.* (2017) 38:447–55. doi: 10.1093/eurheartj/ehv677
58. Aikawa E, Nahrendorf M, Figueiredo J-L, Swirski FK, Shtatland T, Kohler RH, et al. Osteogenesis associates with inflammation in early-stage atherosclerosis evaluated by molecular imaging *in vivo*. *Circulation.* (2007) 116:2841–50. doi: 10.1161/CIRCULATIONAHA.107.732867
59. Aikawa E, Nahrendorf M, Sosnovik D, Lok VM, Jaffer FA, Aikawa M, et al. Multimodality molecular imaging identifies proteolytic and osteogenic activities in early aortic valve disease. *Circulation.* (2007) 115:377–86. doi: 10.1161/CIRCULATIONAHA.106.654913
60. Zaheer A, Lenkinski RE, Mahmood A, Jones AG, Cantley LC, Frangioni JV. *In vivo* near-infrared fluorescence imaging of osteoblastic activity. *Nat Biotechnol.* (2001) 19:1148–54. doi: 10.1038/nbt1201-1148
61. Derwall M, Malhotra R, Lai CS, Beppu Y, Aikawa E, Seehra JS, et al. Inhibition of bone morphogenetic protein signaling reduces vascular calcification and atherosclerosis. *Arterioscler Thromb Vasc Biol.* (2012) 32:613–22. doi: 10.1161/ATVBAHA.111.242594

62. Figueiredo J-L, Aikawa M, Zheng C, Aaron J, Lax L, Libby P, et al. Selective cathepsin S inhibition attenuates atherosclerosis in apolipoprotein E-deficient mice with chronic renal disease. *Am J Pathol.* (2015) 185:1156–66. doi: 10.1016/j.ajpath.2014.11.026
63. Shi X, Gao J, Lv Q, Cai H, Wang F, Ye R, et al. Calcification in atherosclerotic plaque vulnerability: friend or foe? *Front Physiol.* (2020) 11:56. doi: 10.3389/fphys.2020.00056
64. Abran M, Stähli BE, Merlet N, Mihalache-Avram T, Mecteau M, Rhéaume E, et al. Validating a bimodal intravascular ultrasound (IVUS) and near-infrared fluorescence (NIRF) catheter for atherosclerotic plaque detection in rabbits. *Biomed Opt Express.* (2015) 6:3989–99. doi: 10.1364/BOE.6.003989
65. Maehara A, Matsumura M, Ali ZA, Mintz GS, Stone GW. IVUS-guided versus OCT-guided coronary stent implantation: a critical appraisal. *JACC Cardiovasc Imaging.* (2017) 10:1487–503. doi: 10.1016/j.jcmg.2017.09.008
66. Yoo H, Kim JW, Shishkov M, Namati E, Morse T, Shubochkin R, et al. Intra-arterial catheter for simultaneous microstructural and molecular imaging *in vivo*. *Nat Med.* (2011) 17:1680–4. doi: 10.1038/nm.2555
67. Bourantas CV, Jaffer FA, Gijzen FJ, van Soest G, Madden SP, Courtney BK, et al. Hybrid intravascular imaging: recent advances, technical considerations, and current applications in the study of plaque pathophysiology. *Eur Heart J.* (2017) 38:400–12. doi: 10.1093/eurheartj/ehw097
68. Lee S, Lee MW, Cho HS, Song JW, Nam HS, Oh DJ, et al. Fully integrated high-speed intravascular optical coherence tomography/near-infrared fluorescence structural/molecular imaging *in vivo* using a clinically available near-infrared fluorescence-emitting indocyanine green to detect inflamed lipid-rich atheromata in coronary-sized vessels. *Circ Cardiovasc Interv.* (2014) 7:560–9. doi: 10.1161/CIRCINTERVENTIONS.114.001498
69. Kim S, Lee MW, Kim TS, Song JW, Nam HS, Cho HS, et al. Intracoronary dual-modal optical coherence tomography-near-infrared fluorescence structural-molecular imaging with a clinical dose of indocyanine green for the assessment of high-risk plaques and stent-associated inflammation in a beating coronary artery. *Eur Heart J.* (2016) 37:2833–44. doi: 10.1093/eurheartj/ehv726
70. Potkin BN, Bartorelli AL, Gessert JM, Neville RF, Almagor Y, Roberts WC, et al. Coronary artery imaging with intravascular high-frequency ultrasound. *Circulation.* (1990) 81:1575–85. doi: 10.1161/01.CIR.81.5.1575
71. Dixon AJ, Hossack JA. Intravascular near-infrared fluorescence catheter with ultrasound guidance and blood attenuation correction. *J Biomed Opt.* (2013) 18:56009. doi: 10.1117/1.JBO.18.5.056009
72. Abran M, Cloutier G, Cardinal M-HR, Chayer B, Tardif J-C, Lesage F. Development of a photoacoustic, ultrasound and fluorescence imaging catheter for the study of atherosclerotic plaque. *IEEE Trans Biomed Circuits Syst.* (2014) 8:696–703. doi: 10.1109/TBCAS.2014.2360560
73. Bozhko D, Osborn EA, Rosenthal A, Verjans JW, Hara T, Kellnberger S, et al. Quantitative intravascular biological fluorescence-ultrasound imaging of coronary and peripheral arteries *in vivo*. *Eur Heart J Cardiovasc Imaging.* (2017) 18:1253–61. doi: 10.1093/ehjci/jew222
74. Li Y, Jing J, Qu Y, Miao Y, Zhang B, Ma T, et al. Fully integrated optical coherence tomography, ultrasound, and indocyanine green-based fluorescence tri-modality system for intravascular imaging. *Biomed Opt Express.* (2017) 8:1036–44. doi: 10.1364/BOE.8.001036
75. Ughi GJ, Wang H, Gerbaud E, Gardecki JA, Fard AM, Hamidi E, et al. Clinical characterization of coronary atherosclerosis with dual-modality OCT and near-infrared autofluorescence imaging. *JACC Cardiovasc Imaging.* (2016) 9:1304–14. doi: 10.1016/j.jcmg.2015.11.020
76. Htun NM, Chen YC, Lim B, Schiller T, Maghazal GJ, Huang AL, et al. Near-infrared autofluorescence induced by intraplaque hemorrhage and heme degradation as marker for high-risk atherosclerotic plaques. *Nat Commun.* (2017) 8:75. doi: 10.1038/s41467-017-00138-x
77. Burton NC, Patel M, Morscher S, Driessen WHP, Claussen J, Beziere N, et al. Multispectral opto-acoustic tomography (MSOT) of the brain and glioblastoma characterization. *Neuroimage.* (2013) 65:522–8. doi: 10.1016/j.neuroimage.2012.09.053
78. Wang B, Karpouk A, Yeager D, Amirian J, Litovsky S, Smalling R, et al. *In vivo* intravascular ultrasound-guided photoacoustic imaging of lipid in plaques using an animal model of atherosclerosis. *Ultrasound Med Biol.* (2012) 38:2098–103. doi: 10.1016/j.ultrasmedbio.2012.08.006
79. Iskander S. *In vivo* intravascular photoacoustic imaging of plaque lipid in coronary atherosclerosis. *Eurointervention.* (2019) 15:452–6. doi: 10.4244/EIJ-D-19-00318
80. Vinegoni C, Botnaru I, Aikawa E, Calfon MA, Iwamoto Y, Folco EJ, et al. Indocyanine green enables near-infrared fluorescence imaging of lipid-rich, inflamed atherosclerotic plaques. *Sci Transl Med.* (2011) 3:84ra45. doi: 10.1126/scitranslmed.3001577
81. Verjans JW, Osborn EA, Ughi GJ, Calfon Press MA, Hamidi E, Antoniadis AP, et al. Targeted near-infrared fluorescence imaging of atherosclerosis: clinical and intracoronary evaluation of indocyanine green. *JACC Cardiovasc Imaging.* (2016) 9:1087–95. doi: 10.1016/j.jcmg.2016.01.034
82. Osborn EA, Ughi GJ, Verjans JW, Gerbaud E, Takx RA, Tawakol A, et al. Abstract 656: *in vivo* plaque inflammation and endothelial permeability independently predict atherosclerosis progression: a serial multimodality imaging study arteriosclerosis, thrombosis, and vascular biology. *Arterioscler Thromb Vasc Biol.* (2016) 36:A656.

Conflict of Interest: FAJ has received sponsored research grants from Canon and Siemens; he is a consultant for Boston Scientific, Abbott Vascular, Siemens, Acrostak, and Biotronik. Massachusetts General Hospital has a patent licensing arrangement with Canon, and FAJ has the right to receive royalties.

The remaining author declares that the research was conducted in the absence of any commercial or financial relationships that could be construed as a potential conflict of interest.

Copyright © 2020 Khraishah and Jaffer. This is an open-access article distributed under the terms of the Creative Commons Attribution License (CC BY). The use, distribution or reproduction in other forums is permitted, provided the original author(s) and the copyright owner(s) are credited and that the original publication in this journal is cited, in accordance with accepted academic practice. No use, distribution or reproduction is permitted which does not comply with these terms.